Thermo-mechanical analysis of plasma facing components of diagnostics in the Wendelstein 7-X stellarator

M.Y. Ye, M. Hirsch, R. König, M. Laux, H. Thomsen, A. Weller, A. Werner

Max-Planck-Institut fuer Plasmaphyisk, EURATOM Association, Teilinstitut Greifswald, Wendelsteinstr. 1, D-17491 Greifswald, Germany

Abstract

For long-pulse plasma operation of the W7-X stellarator, one of the most serious challenges for the design of in-vessel diagnostic systems is the thermo-mechanical problem. Thermal load from convective losses and from plasma radiation can reach up to 500kW/m^2 at some locations close to plasma. The typical thermal load from plasma radiation alone ranges from 10 to 100 kW/m^2 as derived from 3-D Monte-Carlo simulations. Most plasma facing diagnostic components require active cooling for the long-pulse plasma operation. Especially the design of optical components must be optimized to minimize thermal deformations. Finite element analyses (FEA) are performed for better understanding of thermo-mechanical problems on plasma facing components of diagnostics, and to guide the design of the diagnostic system. As examples the paper presents the FEA results of the Corner-Cube Retro-Reflectors for the CO_2-laser interferometer and the movable pop-up probe arrays in the divertor.

Keywords: W7-X stellarator; Steady state diagnostics; Heat load; Plasma facing components; Thermo-mechanical analysis

PACS: 52.55.Hc, 52.70.-m

1. Introduction

The superconducting stellarator Wendelstein 7-X (W7-X), now under construction in Greifswald, is designed for stationary operation (30 minutes) with continuous wave heating by ECRH with up to 10 MW power, and additional heating by NBI and ICRH with power up to 14 MW for 10s. The actively water cooled divertor target plates and baffles have been designed to withstand heat loads up to 10 MW/m^2 and 1 MW/m^2, respectively [1]. The residual in-vessel area is covered by water cooled panels which are able to remove a power load of 200 kW/m^2 during steady state operation. The thermal loads on

all plasma facing components are 10-100 kW/m^2 from plasma radiation alone [2] or/and ECRH stray radiation levels of 50 – 200 kW/m^2 in high density scenarios [3]. Even outside the divertor additional convective loads on components located close to plasma edge can reach up to 500 kW/m^2. Therefore, the particularly challenging task to design diagnostics compatible with steady state operation is solved by proper shielding and active cooling. Diagnostic components located behind such a heat shield require individual cooling also, as thermal radiation from the cooled but still rather hot shielding components is rather high. In the cases of direct exposure of diagnostic components like mirrors, detectors and windows, the direct radiative thermal loads from the plasma cannot be avoided. For optical components the thermal deformation must be taken into account and should be minimized according to the restriction peculiar to the individual optical component. Therefore, the thermo-mechanical analysis is a critical design step for the design of diagnostic systems under steady state operation.

2. Heat loads on plasma facing components of diagnostics

The design of the plasma facing components of diagnostics needs the consideration of the maximum heat load. A 3-D Monte-Carlo simulation code has been developed to calculate the expected radiative power loads for various assumed radiation profiles: such as centrally peaked, parabolic and edge peaked radiation. The calculated maximum thermal loads from plasma radiation at the entrance of diagnostic ports is about 50 - 70 kW/m^2 [2]. Similar calculations were performed for the radiative heat load inside the ports. The results indicate that the thermal load at a retracted position of 1 m distance to the port entrance is still a few kW/m^2 as shown in Fig. 1. In some cases the direct exposure of diagnostic components, for example the Corner-Cube Retro-Reflectors (CCRs) of the multichannel CO_2-Interferometer diagnostic, to radiative thermal loads of 90 kW/m^2 results in an, for an interferometer unacceptably large, deformation of the reflector surfaces (see section 3). For spectroscopic diagnostics an actively water cooled sapphire window has been designed and tested in the laboratory. It has been shown that the window is able to withstand heat loads of up to 58 kW/m^2 [4]. Diagnostics like the diamagnetic loop or the soft-X-ray multi-camera tomography system (XMCTS) are expected to be additionally exposed to convective loads of up to 500 kW/m^2 due to their proximity to the plasma edge [5]. A special heat shield made of graphite tiles (on the plasma facing side) clamped onto a copper-chromium-zirconium (CuCrZr) heat sink with brazed stainless steel (SS) cooling tubes has been designed to

withstand this heat load of 500 kW/m^2 [6]. In the case of the XMCTS diagnostics, a water cooled heat shield is needed to protect the camera body from high plasma thermal load. Not only the thermal radiation from the hot rear side surfaces of the heat sink with temperatures of ~400^o C, which alone results in thermal loads of ~ 6 kW/m^2, but also the plasma radiation through the observation pinhole in the heat shield contributes significantly to the thermal load onto the detector. Since the Si-detectors require a working temperature below 30^{o}C the cameras still need direct active cooling [6, 7]. For probe diagnostics in the divertor it has been proposed to install movable (pop-up) probe arrays in poloidal gaps between divertor target modules. The probe tips are exposed not only to high thermal loads of about 50 MW/m^2 during the short probe operation, but also to prolonged radiative load form the plasma and hot divertor target at retracted position. The thermal analysis for the probe system is presented in section 4.

3. Corner-Cube Retro-Reflectors

Due to non-planar coils with complex shape and the divertor structures it is not possible to have large ports poloidally opposite to each other [8]. Therefore two diagnostics, the Far Infrared (FIR) Polarimeter and the multichannel CO_2-Interferometer must use Corner-Cube Retro-Reflectors (CCR) for measuring density profiles. The CCR consists of three mutually orthogonal reflecting surfaces which form a corner of a cube and make the reflected beam parallel to an incident beam regardless of the incident angle. The multi-channel CO_2-Laser interferometer requires 11 CCR which have to be integrated in the first wall tiles of the cooled heat shield. Necessarily the CCR aperture itself is directly exposed to the plasma. Expected power flux in standard operation is about 90 kW/m^2 from plasma radiation. For steady state operation the main design challenge is to guarantee the optical requirements for these CCR with respect to surface flatness; in particular that over a laser spot of 8 mm diameter the relative deformation perpendicular to the mirror surface on the three reflector surfaces is fulfilled, namely, that it stays well below 1 μm. The CCR is still in the conceptual design phase with the following main issues which concern the thermo-mechanical design: (a) material selection for CCR, (b) incorporation and cooling of the CCR, and (c) fastening of the CCR with minimum relative deformation of the CCR mirror surfaces.

As its aperture is open to the high temperature plasma the CCR ideally should use low-Z materials. However, the required combination of good heat conductivity and low thermal expansion for the CCR

itself forces to consider molybdenum (Mo) or tungsten (W) as a reflector material. For the first design Mo was used (Fig. 2a). Three plates (6 mm thickness, 18 mm width) were mutually fastened, and one of the three plates was clamped by a SS plate to the CCR housing (possibly made of CuCrZr) as shown in Fig. 2b. The CCR housing is tightly fastened to the heat sinks of the cooled heat shield (Fig. 2c). The optical aperture for the CCR is restricted to 2.54 cm in diameter due to space limitations (Fig. 2d). The design allows removing the CCR for maintenance or cleaning during shutdown. The distance between tile surface directed towards the plasma and the vessel wall is about 35 mm minimum. The finite element thermal analysis was carried out for a heat load of 90 kW/m^2 onto the heat shield and the Mo-CCR reflectors, and with the cooling water temperature fixed at 40 ^oC. Perfect thermal contact between the clamp fastened to one of these Mo-plates and the cooling house was assumed. Figure 3 shows the calculated temperature evolution at selected locations of the components. The temperature of all components reaches the thermal equilibrium after 300 s, and the maximum temperatures are acceptable for materials of the components. The results show that by cooling the maximum temperature of the CCR housing can be limited to 140^o C. The temperature distribution of the fastened CCR is 270^o C - 300^o C, and over the whole CCR surface the temperature range stays within 270^o C < T < 326^o C. The temperature variation over the laser spot (centered at CCR, spot diameter d = 8 mm) is 280^o C < T < 312^o C. For this temperature distribution in the reflectors the mechanical analysis is performed. A heat expansion of 5.1 microns/K at room temperature, a Young modulus of 324.8 GPa and a Poisson ratio of 0.3 were used for the Mo material. The interfaces of the reflectors were assumed as a fixed boundary condition. The calculated results show that for this design the deformation perpendicular to mirror surfaces of the reflectors is 0-10 μm over a laser spot of 8 mm diameter. In order to confirm whether such deformation resulted from an inhomogeneous surface temperature distribution, a FE analysis was also performed for the case when each of the three reflectors was cooled to 270^o C at its rear sides (this back surface temperature being derived from the single reflector cooling). As a result the surface temperatures then became rather homogenous. Over the laser spot the temperature then varies by only < 2^o C around the 272^o C level. However, the relative deformation perpendicular to mirror surface is still 0 - 7 μm. Therefore this deformation is mainly determined by the mutual stiffness of the fastened CCR plates.

As a consequence second design aimed to minimise thermal mechanical stresses. The geometry of the Mo-CCR was improved by introducing appropriate slits between the reflector plates to allow for their free thermal expansion as shown in Fig. 4a. The geometry of one reflector plate is shown in Fig. 4b. The distance between top surface (mirror surface) and bottom surface (interface to cooling structure) varies from 3 mm to 21mm, which is different from the uniform thickness of the reflector in the first design. For symmetry reasons the three Mo-reflectors are fastened at the bottom to a Mo-plate (not shown), which are all together fastened to the CuCrZr housing. Optimisation of the cooling and fastening for the CCR has been performed with FE analysis for a single reflector only. The uniform heat load of 90 kW/m^2 was applied onto the top surface of the reflector, and cooling and fastening was selected at the bottom of the reflector. The FE analytical results indicate that the relative deformation of the mirror surface is very sensitive to the fastening condition at the bottom. It is found that the reflector bottom mechanically fixed at the small region of the bottom edge only is the optimum solution for this design. Figure 5a shows the temperature distribution in the reflector. The blue area at the bottom is the fastening area in which the temperature was fixed at 270^o C as cooling condition in the thermal analysis, and the displacement was fixed as boundary condition in the mechanical analysis. The temperature range over whole reflector is 270^o C < T < 293^o C. The temperature variation across the mirror surface becomes 286^o C < T < 293^o C. For this temperature distribution the deformation of the reflector is calculated. Figure 5b shows the displacement distribution of the reflector in the direction perpendicular to the mirror surface. Figs. 6a and b show the displacement profile along the diagonal line from A to B and from C to D indicated in Fig. 4b. Over the whole mirror surface the displacement range is 18.2 μm - 21.7 μm. Although the maximum relative deformation of the whole surface is about 3 μm, the deformation over a laser spot of 8 mm diameter centred at the mirror surface is less than 1 μm (Fig. 6b). Therefore it is concluded that the cooling and fastening interface close to the bottom edge results not only in a small temperature variation across the top surface, but also allows to minimize the impact of the stresses.

3. Probe arrays within the divertor

Target-integrated arrays of electrostatic Langmuir probes are usually used to measure basic plasma parameters close to the divertor targets. Such probes have to withstand the same or even higher thermal loads than the divertor target plates themselves. This means that, for long-pulse or steady-state operation,

fixed probe tips have to be flush mounted and actively cooled. This solution could result in problems with interpretation of probe characteristics due to very shallow angles of incidence between flush-mounted probe surfaces and magnetic field lines. Beside this, cooling equipments for a large number of probes would, according to the present divertor concept, spatially interfere with the target cooling supply. In order to avoid these problems it has been proposed to install movable (pop-up) probe arrays without active cooling and with the tips repeatedly, but shortly exposed to the divertor plasma [9]. The arrays (32 probe tips per array) have to be fitted into poloidal gaps between target modules. The probe tip with an oblique plane front face at an angle of about 10^o with respect to the magnetic field is expected to be exposed to a heat load of about 50 MW/m^2 (convection and conduction) at an exposure position of 2 mm in front of the target surface for a time interval of 50 ms. On the other hand, the retracted position of the probe tip should exclude direct heat load parallel to the field lines as well as perpendicular load due to anomal transport. A stand-by position of ≈ 3 mm behind the target surface seems to be adequate. However, the probe is still heated by the thermal radiation from both the plasma and the hot divertor target at stand-by position during 30 minutes steady state operation. In order to avoid a thermal overload, the thermal behaviour of the probe arrays has been investigated based on the present concept design.

A simplified 3D FE model was created for the thermal analysis of the probe as shown in Fig. 7. The model consists of a CFC cylindrical tip (diameter of 3 mm, 55 mm length), an AlN cylindrical tube (thickness 1 mm, 55 mm length) for insulation, a Mo-tube (thickness 1 mm, 40 mm length) for shielding, Al or graphite tube (thickness 2.5 mm, 24 mm length) for probe supporting, and the divertor target simplified into a cylinder around the probe tip. For the FE analysis the target was considered to have a steady temperature distribution encompassing six areas with fixed average temperatures of 750^o C, 500^o C, 300^o C, 200^o C, 100^o C, and 60^o C, respectively. The location and extend of the areas was derived from FE calculations of the temperature distribution in the water-cooled divertor target under a thermal load of 10 MW/m^2 during steady-state operation. A heat load of 50 MW/m^2 onto the front surfaces of CFC tip and AlN tube is assumed at the exposure position, and about 50 kW/m^2 from plasma radiation at stand-by position 3 mm behind the target surface. No thermal contact is assumed between any parts, the heat exchange among components is only by radiation. The temporal temperature distribution is calculated by ANSYS code for different exposure times and frequencies. The materials properties for calculations are listed in table 1. Figure 8a shows the temperature evolution at selected positions of components in the

case of a 50 ms exposure time and 30 minutes of stand-by. The temperature evolution of the AlN tube shows a similar thermal behaviour to the CFC tip (not shown). During the 50 ms exposure to a high heat load of 50 MW/m^2 the peak temperatures of the front surfaces of the CFC tip and of the AlN tube rapidly reach temperature of 608^o C and 654^o C, respectively. Afterwards a heat load of 50 kW/m^2 remains for 30 minutes. During this period the average temperature gradually increases and reaches an equilibrium temperature of 482^o C. The temperature of the Mo shield reaches 297^o C due to the radiation heat exchange with the AlN tube and target. The temperature of the Al support reaches 65^o C by thermal radiation from the Mo shield. Figure 8b shows the temperature evolution for 30 cycles at selected component positions for 50 ms exposure time, and 60 s retracted at stand-by position. The peak temperature of the CFC tip arrives at a saturated value of about 1060^o C after exposure to 30 cycles and the temperature over the whole CFC tip and AlN tube reaches an equilibrium temperature of 580^o C at stand-by position. The temperature of the Mo shield and Al support reaches 380^{o}C and 110^{o}C, respectively. Moreover, FE calculations were performed for different emissivities of the AlN tube. These results indicate that the average temperature can be reduced by ~30% for the AlN tube if the emissivity is changed from 0.1 to 0.6. The temperature at the CFC tip could correspondingly be decreased by 15% only.

4. Summary

FE thermal-mechanical analyses have been carried out for the design of main in-vessel diagnostics. For Corner-Cube Retro-Reflectors (CCR) main deformation arrives from the internal stiffness of the structure. Thermo-mechanical analyses indicate that in order to allow for a homogenous surface temperature and additionally reduce stress the CCR structure should be designed as high (massive) as possible within the allowable space, and the fastening interface should be as distant as possible from the mirror surface. In order to verify the accuracy of the model calculations, appropriate tests for the CCR are needed and are under discussion. Further FE analyses will be performed for the design of the CCR in realistic geometry, for in-homogenous heat loads, and different fastening structures as well as materials. For the planned pop-up probe arrays a fast back and forth motion is absolutely necessary to avoid overheating of the measuring system. As main result of the FE calculations it can be concluded that for

movable probe arrays relying on inertial cooling the temperatures of all components remain in the acceptable range. Further thermal analyses will include a realistic support structure.

Acknowledgements

The authors wish to thank Dr. F. Schauer and Mr. V. Bykov for their discussion.

References:

[1] H. Greuner, B. Böswirth, J. Boscary, G. Hofmann, B. Mendelevitch, H. Renner, et al., Final design of W7-X divertor plasma facing components tests and thermo-mechanical analysis of baffle prototypes, Fusion Eng. Des. 66-68 (2003) 447-452.

[2] T. Eich, A. Werner, Numerical studies on radiative heat load to plasma facing components for W7-X stellarator, Fusion Sci. Technol. 53 (2008) 761-779

[3] H.-J. Hartfuß, R. König , A. Werner, Diagnostics for steady state plasmas, Plasma Phys. Control. Fusion 48 (2006) R83- R150

[4] R. König, J. Cantarini, H. Dreier, V. Erckmann, D. Hildebrandt, M. Hirsch, et al., Diagnostic developments for quasi- continuous operation of the Wendelstein 7-X stellarator, Rev. Sci. Instrum. 79, (2008) 10F337-1-4.

[5] A. weller, S. Mohr, C. Junghans, Concepts of x-ray diagnostics for Wendelstein 7-X, Rev. Sci. Intrum. 75 (2004) 3962-3965

[6] M.Y. Ye, A. Werner, M. Hirsch, A. Weller, H. Thomsen, R. König, Thermal-mechanical analysis for in-vessel diagnostic components in W7-X, AIP Conf. Proc. 993 (2008) 211-214

[7] H. Thomsen, T. Broszat, P. Carvalho, S. Mohr, A. Weller, M.Y. Ye, The steady state challenge for soft x-ray diagnostics on Wendelstein 7-X stellarator, AIP Conf. Proc. 993 (2008) 163-166

[8] P. Kornejew, M. Hirsch, T. Bindemann, A. Dinklage, H. Dreier, H.-J. Hartfuß. Design of multichannel laser interometry for W-7X, Rev. Sci. Instrum. 77 (2006) 10F128-1-3

[9] M. Laux, P. Grigull, H.Greve, A. Reichert, J. Sachtleben, M.Y. Ye, Probe systems for W7-X, Contrib. Plasma Phys. 46 (2006) 392 – 398

Figure/table Captions

Figure 1. 3D Monte-Carlo calculation of radiative heat loads on surfaces perpendicular to port axis inside ports. AEA and AEF are port names in W7-X. The inset figure shows radiation profile.

Figure 2. FE Model of conceptual design for retro-reflectors integrated within heat shield. (a) CCR consists of three reflectors which are mutually orthogonal. (b) CCR is incorporated into CuCrZr housing. (c) The CCR housing is tightly fastened to the heat sinks of the cooled heat shield. (d) View onto the heat protection from plasma side.

Figure 3. FE calculated temperature evolution at selected locations of the components.

Figure 4. (a) Improved geometry of the CCR with appropriate slits between reflectors indicated by arrows. (b) The geometry of one reflector. The length of the line AB is 21.6mm, the line CD is 29.2mm, and the lines AC and AD are 20.7mm.

Figure 5. FE calculation results. (a) Equilibrium temperature distribution of the reflector. The temperature in the blue area was fixed at 270 ^{o}C as cooling condition. (b) Displacement distribution of the reflector in the direction perpendicular to the mirror surface.

Figure 6. Surface deformation perpendicular to the mirror surface. (a) Profile of the displacement along the diagonal line from A to B. (b) Profile of the displacement along the diagonal line from C to D.

Figure 7. Langmuir Probe model for FE calculation. (a) Model overview. (b) View of the probe with divertor target and Al support removed.

Figure 8. Temperature evolution of the Langmuir probe components. (a) In the case of 50 ms exposed time and 30 minutes at stand-by position. (b) In the case of 50 ms exposed time for 30 cycles with 60 s at stand-by position.

Table 1 Material properties

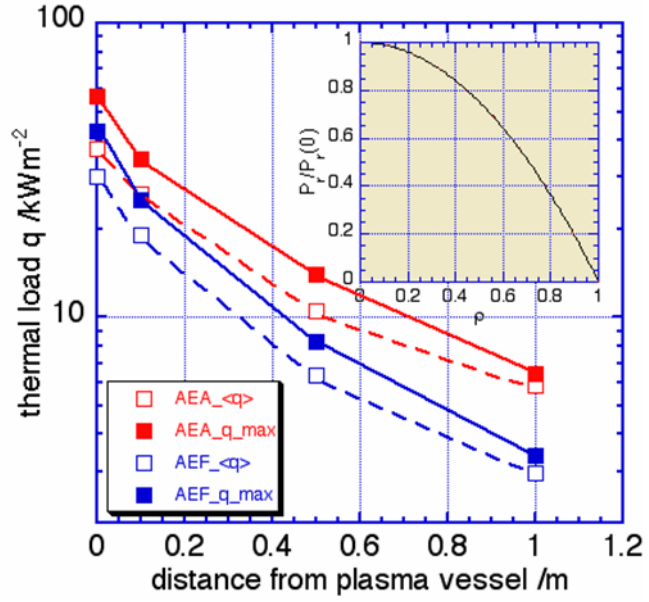

Figure 1. 3D Monte-Carlo calculation of radiative heat loads on surfaces perpendicular to port axis inside ports. AEA and AEF are port names in W7-X. The inset figure shows radiation profile.

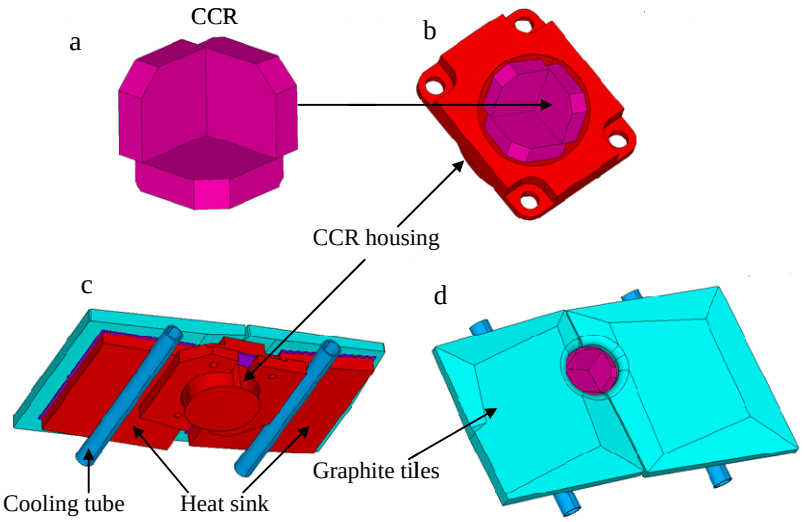

Figure 2. FE Model of conceptual design for retro-reflectors integrated within heat shield. (a) CCR consists of three reflectors which are mutually orthogonal. (b) CCR is incorporated into CuCrZr housing. (c) The CCR housing is tightly fastened to the heat sinks of the cooled heat shield. (d) View onto the heat protection from plasma side.

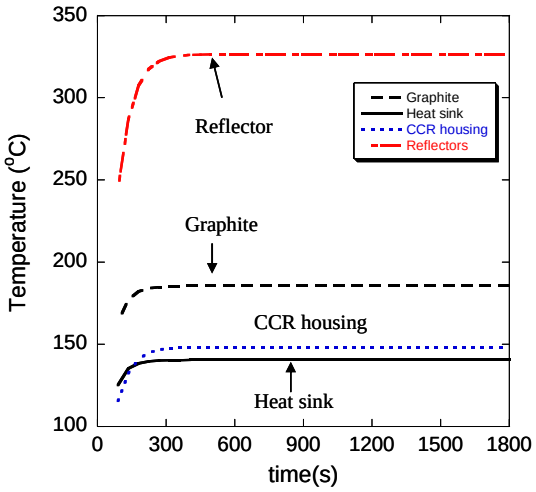

Figure 3. FE calculated temperature evolution at selected locations of the components.

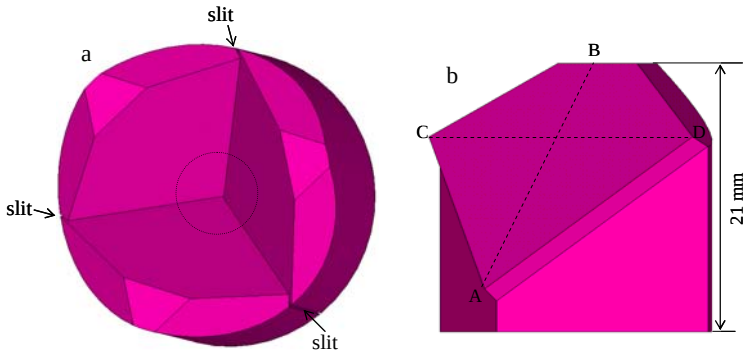

Figure 4. (a) Improved geometry of the CCR with appropriate slits between reflectors indicated by arrows. (b) The geometry of one reflector. The length of the line AB is 21.6mm, the line CD is 29.2mm, and the lines AC and AD are 20.7mm.

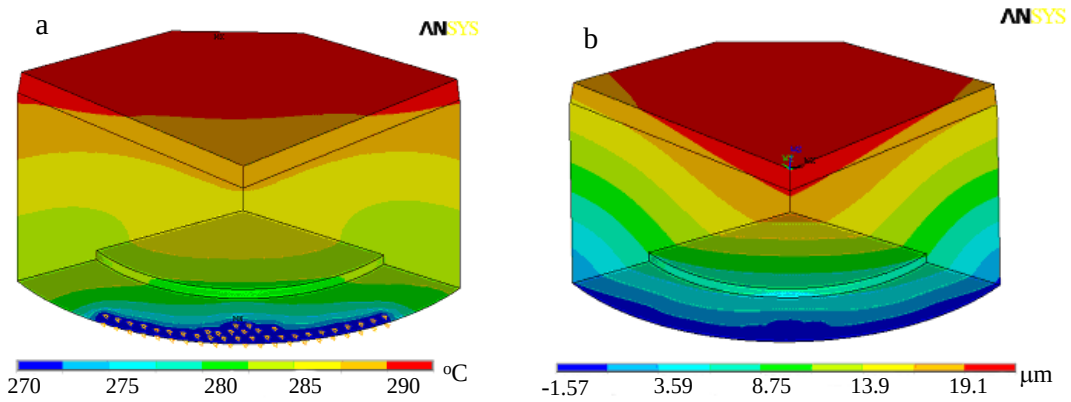

Figure 5. FE calculation results. (a) Equilibrium temperature distribution of the reflector. The temperature in the blue area was fixed at 270 °C as cooling condition. (b) Displacement distribution of the reflector in the direction perpendicular to the mirror surface.

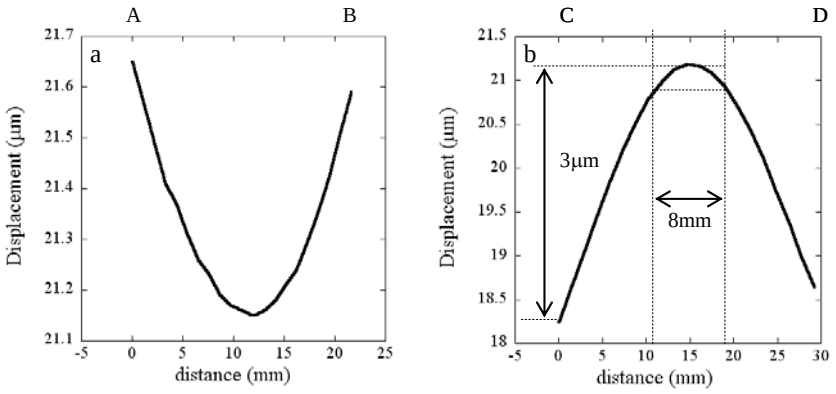

Figure 6. Surface deformation perpendicular to the mirror surface. (a) Profile of the displacement along the diagonal line from A to B. (b) Profile of the displacement along the diagonal line from C to D.

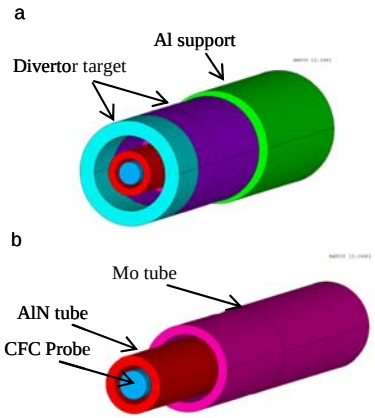

Figure 7. Langmuir Probe model for FE calculation. (a) Model overview. (b) View of the probe with divertor target and Al support removed.

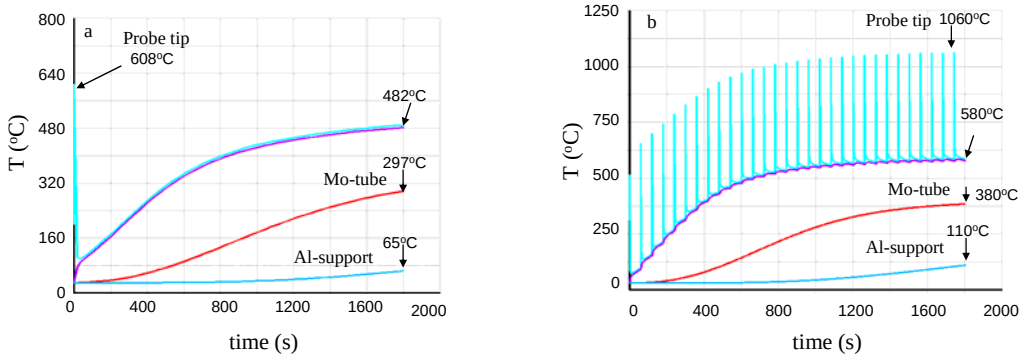

Figure 8. Temperature evolution of the Langmuir probe components. (a) In the case of 50 ms exposed time and 30 minutes at stand-by position. (b) In the case of 50 ms exposed time for 30 cycles with 60 s at stand-by position.

Table 1
Material properties

Components	Density (kg/m^3)	Heat capacity (J/kg_K)	Heat conductivity (W/m_K)	Emissivity
CFC probe	1800	T dependent	200	0.8
AlN tube	3330	800	150	0.3
Mo tube	10240	251	138	0.1
Al support	2700	900	237	0.5